

## Nuclear Structure Aspects of Neutrinoless Double- $\beta$ Decay

B. A. Brown,<sup>1</sup> M. Horoi,<sup>2</sup> and R. A. Sen'kov<sup>2,3</sup>

<sup>1</sup>*Department of Physics and Astronomy and National Superconducting Cyclotron Laboratory, Michigan State University, East Lansing, Michigan 48824-1321, USA*

<sup>2</sup>*Department of Physics, Central Michigan University, Mount Pleasant, Michigan 48859, USA*

<sup>3</sup>*Department of Natural Sciences, LaGuardia Community College, The City University of New York, Long Island City, New York 11101, USA*

(Received 25 September 2014; published 22 December 2014)

We decompose the neutrinoless double- $\beta$  decay matrix elements into sums of products over the intermediate nucleus with two less nucleons. We find that the sum is dominated by the  $J^\pi = 0^+$  ground state of this intermediate nucleus for both the light and heavy neutrino decay processes. This provides a new theoretical tool for comparing and improving nuclear structure models. It also provides the connection to two-nucleon transfer experiments.

DOI: 10.1103/PhysRevLett.113.262501

PACS numbers: 23.40.Bw, 21.60.Cs, 23.40.Hc, 14.60.Pq

Many properties of the active neutrinos are measured, but it is not yet established whether they are Dirac or Majorana type particles and their absolute masses are not known. Left-right symmetric extensions to the standard model provide an explanation for the nonzero masses of the left-handed light neutrinos and also predict the existence of right-handed heavy neutrinos [1]. Neutrinoless double- $\beta$  ( $0\nu\beta\beta$ ) decay of nuclei provides unique information on these neutrino properties [2–4]. The  $0\nu\beta\beta$  decay process and the associated nuclear matrix elements (NME) were investigated by using several approaches including the quasiparticle random phase approximation (QRPA) [2], the interacting shell model [5,6], the interacting boson model (IBM) [7,8], the generator coordinate method [9], and the projected Hartree-Fock Bogoliubov model [10]. It is critical to assess which nuclei are the best candidates for experimental study.

Assuming contributions from the light left-handed ( $\nu$ ) neutrino-exchange mechanism and the heavy right-handed ( $N$ ) neutrino-exchange mechanism, the decay rate of a neutrinoless double- $\beta$  decay process can be written as [2,6]

$$[T_{1/2}^{0\nu}]^{-1} = G^{0\nu} (|M_\nu^{0\nu}|^2 |\eta_\nu|^2 + |M_N^{0\nu}|^2 |\eta_N|^2), \quad (1)$$

where  $G^{0\nu}$  is the phase space factor for this decay mode [11,12],  $M^{0\nu}$  are the nuclear matrix elements (NME), and  $\eta_{\nu,N}$  are the neutrino physics parameters [2,6].

Since the experimental decay rate is proportional to the square of the calculated nuclear matrix elements, it is important to calculate these matrix elements with high accuracy to be able to extract the neutrino effective mass which can be used to determine the absolute scale of neutrino masses [Eq. (1) can also be used to identify the dominant decay mechanism [13]]. However, the theoretical methods used give results that differ from one another by factors of up to 2–3. It is important to understand the

nuclear structure aspects of these matrix elements and why the models give differing results. Previously, the structure dependence of the NME have been analyzed in terms of the “charge-exchange” matrix elements with in the same mass chain, as illustrated for the decay of  $^{76}\text{Ge}$  by the intermediate nucleus  $^{76}\text{As}$  in Fig. 1, where a wide range of intermediate state spins are important (see, for example, Figs. 1 and 6 in [14]).

In this Letter we present a new theoretical tool for understanding  $0\nu\beta\beta$  matrix elements by expanding them in terms of a summation over states in the nucleus with two less nucleons ( $A - 2$ ), as shown by the example of  $^{74}\text{Ge}$  in Fig 1. The dependence on the intermediate state angular momenta have been previously discussed [14–16]. We show that the NME are dominated by the contribution through the  $J^\pi = 0^+$  ground state of the ( $A - 2$ ) intermediate nucleus. This opens up new ways of comparing theoretical models and comparing to other experimental data to improve the accuracy of the NME for  $0\nu\beta\beta$  decay.

The  $0\nu\beta\beta$  process can be naturally described in 2nd order perturbation theory, in which the energies of the virtual states of the intermediate nucleus  $^{76}\text{As}$  obtained by a single- $\beta$  decay of the parent nucleus enter into the propagator. However, it has been known for some time (see, e.g., [16,17], and references therein) that these energies are

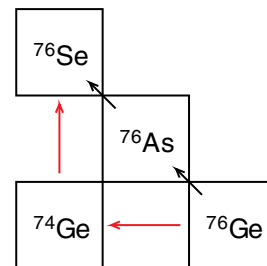


FIG. 1 (color online). Nuclei involved in the calculations for the double- $\beta$  decay of  $^{76}\text{Ge}$ .

small compared to the neutrino exchange energy, and therefore the widely used closure approximation replaces these energies by a constant value and sums out the contribution of the intermediate states. It was shown [14,16,17] that this approximation provides matrix elements about 10% smaller. We recently found [14,16] optimal closure energies for which the nuclear matrix elements in both approaches are the same (see, e.g., Fig. 5 of Ref. [14]). Therefore in this Letter, for the light neutrino exchange matrix elements we use closure approximation with the optimal closure energies, which are 0.5, 3.5, and 3.5 MeV for  $^{48}\text{Ca}$ ,  $^{76}\text{Ge}$ , and  $^{82}\text{Se}$ , respectively. The heavy neutrino exchange matrix elements [2,6] do not depend on the energies of the intermediate states.

The nuclear matrix element  $M^{0\nu}$  can be presented as a sum of Gamow-Teller ( $M_{\text{GT}}^{0\nu}$ ), Fermi ( $M_F^{0\nu}$ ), and tensor ( $M_T^{0\nu}$ ) matrix elements (see, for example, Refs. [16,18]),

$$M^{0\nu} = M_{\text{GT}}^{0\nu} - \left(\frac{g_V}{g_A}\right)^2 M_F^{0\nu} + M_T^{0\nu}, \quad (2)$$

where  $g_V$  and  $g_A$  are the vector and axial constants, correspondingly. In our calculations we use  $g_V = 1$  and  $g_A = 1.254$ . The  $M_\alpha^{0\nu}$  are matrix elements of scalar two-body potentials. The most important are the Gamow-Teller matrix element that has the form  $V_{\text{GT}}(r, A, \mu)\sigma_1 \cdot \sigma_2 \tau_1^- \tau_2^-$  and the Fermi matrix element that has the form  $V_F(r, A, \mu)\tau_1^- \tau_2^-$ , where  $\tau^-$  are the isospin lowering operators. The neutrino potentials depend on the relative distance between the two decaying nucleons  $r$ , the mass number  $A$ , and the closure energy  $\mu$  discussed above. The radial forms are given explicitly [16]. For the heavy-neutrino exchange, the potential does not depend on  $\mu$  and it looks like a smeared-out delta function [2,6].

The matrix element for a scalar two-body operator between an initial state  $|i\rangle = |n, \omega_i, J\rangle$  and final state  $|f\rangle = |n, \omega_f, J\rangle$  of the  $n$ -particle wave function can be expressed in the form of a product over two-body transition densities (TBTD) times two-particle matrix elements

$$\langle f|V|i\rangle = \sum_{J_0, k_\alpha \leq k_\beta, k_\gamma \leq k_\delta} \text{TBTD}(f, i, k, J_0) \langle k_\alpha, k_\beta, J_0|V|k_\gamma, k_\delta, J_0\rangle, \quad (3)$$

where the  $k$  stands for the set of spherical quantum numbers  $(n, \ell, j)$ . The TBTD are given by

$$\text{TBTD}(f, i, k, J_0) = \langle f|[A^+(k_\alpha, k_\beta, J_0) \otimes \tilde{A}(k_\gamma, k_\delta, J_0)]^{(0)}|i\rangle, \quad (4)$$

where  $A^+$  is a two-particle creation operator of rank  $J_0$ ,

$$A^+(k_\alpha, k_\beta, J_0, M_0) = \frac{[a^+(k_\alpha) \otimes a^+(k_\beta)]_{M_0}^{J_0}}{\sqrt{(1 + \delta_{k_\alpha, k_\beta})}}, \quad (5)$$

and  $\tilde{A}(k_\alpha, k_\beta, J_0) = (-1)^{J_0 - M_0} A^+(k_\alpha, k_\beta, J_0, -M_0)$ . One can evaluate the TBTD by inserting a complete set of states for the  $(n-2)$  nucleon system

$$\begin{aligned} \text{TBTD}(f, i, k, J_0) &= \sum_m \frac{\langle f|A^+(k_\alpha, k_\beta, J_0)|m\rangle \langle m|\tilde{A}(k_\gamma, k_\delta, J_0)|i\rangle}{(2J+1)} \\ &= \sum_m \text{TNA}(f, m, k_\alpha, k_\beta, J_0) \text{TNA}(i, m, k_\gamma, k_\delta, J_0), \end{aligned} \quad (6)$$

where  $m$  stands for the quantum numbers  $(\omega_m, J_m)$  of the intermediate state with  $n-2$  nucleons.  $J_0 = J_m$  when  $J = 0$ . The TNA are the two-nucleon transfer amplitudes given by

$$\text{TNA}(f, m, k_\alpha, k_\beta, J_0) = \frac{\langle f|A^+(k_\alpha, k_\beta, J_0)|m\rangle}{\sqrt{(2J+1)}}. \quad (7)$$

The TNA are normalized such that the sum of the TNA<sup>2</sup> over all states in the  $n-2$  nucleon system is  $n_p(n_p-1)/2$  for the removal of two protons and  $n_n(n_n-1)/2$  for the removal of two neutrons, where  $n_{p(n)}$  are the total number of proton (neutrons) in the model space.

We will analyze the  $0\nu\beta\beta$  matrix elements in terms of their dependence on the intermediate states

$$M^{0\nu}(E_x, J_m) = \sum_{E_m < E_x, J_m} V(f, i, m), \quad (8)$$

where

$$\begin{aligned} V(f, i, m) &= \sum_{k_\alpha \leq k_\beta, k_\gamma \leq k_\delta} \langle k_\alpha, k_\beta, J_m|V|k_\gamma, k_\delta, J_m\rangle \\ &\times \text{TNA}(f, m, k_\alpha, k_\beta, J_0) \text{TNA}(i, m, k_\gamma, k_\delta, J_0). \end{aligned} \quad (9)$$

The results for  $^{48}\text{Ca}$  were obtained for the  $pf$  model space with the set of four orbitals  $(0f_{7/2}, 0f_{5/2}, 1p_{3/2}, 1p_{1/2})$  for both protons and neutrons. We use the GXPF1A Hamiltonian [19] for the  $pf$  model space. The results for  $^{76}\text{Ge}$  and  $^{82}\text{Se}$  were obtained in the  $jj44$  model space with the set of four orbitals  $(0f_{5/2}, 1p_{3/2}, 1p_{1/2}, 0g_{9/2})$  for both protons and neutrons. We use the JUN45 Hamiltonian [20] for the  $jj44$  model space. We use the shell-model computer code NUSHELLX [21].

The results for  $^{76}\text{Ge}$  are shown in Fig. 2 where the running sum, Eq. (8), is shown as a function of the excitation energy and intermediate spin values  $J_m$  in  $^{74}\text{Ge}$ . The red dot shows the result obtained directly from

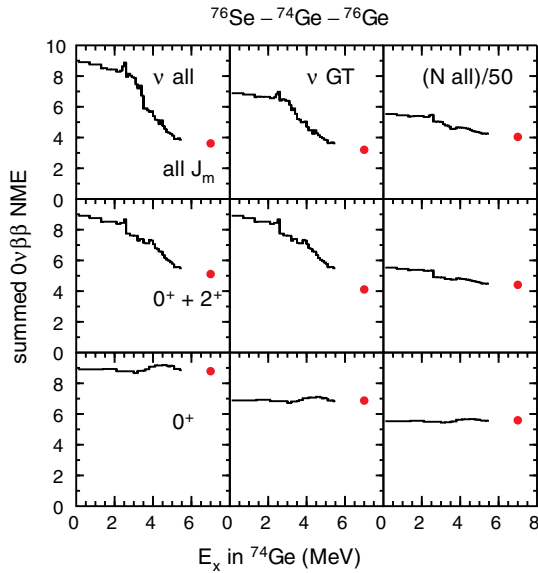


FIG. 2 (color online). Results for  $^{76}\text{Ge}$ . The left-hand column shows the light-neutrino results ( $\nu$ ) for the sum of the GT,  $F$ , and  $T$  contributions. The middle column shows the light-neutrino results for the GT contribution only. The right-hand column shows the heavy-neutrino results ( $N$ ) for the sum of the GT,  $F$ , and  $T$  contribution. The bottom row shows the running sums for the  $0^+$  intermediate states. The middle row shows the running sums for the  $0^+$  and  $2^+$  intermediate states. The top row shows the running sums for all intermediate states. The red dots are the exact results for the sum over all intermediate states.

Eq. (3) using closure with the optimal closure energy (equivalent to the sum over all intermediate states in  $^{76}\text{As}$ ). We include 20 intermediate states for each  $J_m$  except for  $J_m^\pi = 2^+$  where we include 50 states. This number of intermediate states goes up to about 6 MeV in excitation in  $^{74}\text{Ge}$ . We find that the NME is dominated by the contribution through the  $J_m^\pi = 0^+$  ground state of  $^{74}\text{Ge}$ —the large NME at  $E_x = 0$  in Fig. 2. This is a remarkable and simplifying result. It means that the nuclear structure aspects of this dominant term are related to the rather well-studied pair transfer properties of the nuclear ground states. It is a consequence of the strong pairing interaction in the nuclear Hamiltonian. There are cancellations from intermediate states with  $J_m > 0$  up to about 6 MeV in excitation that are dominated by the  $2^+$  contributions. This cancellation reduces the total matrix element by about a factor of 2 for light neutrinos and about 20% for heavy neutrinos.

The results for  $^{48}\text{Ca}$  and  $^{82}\text{Se}$  are shown in Figs. 3 and 4, respectively. Here we present the results for CD-Bonn short range correlations [18]. Numerical results can be found in Refs. [14,16]. The overall patterns are the same as seen for  $^{76}\text{Ge}$ . The results for  $^{48}\text{Ca}$  are particularly simple with 80% of the total matrix elements coming from just the  $0^+$  ground state and the first excited  $2^+$  state. We have also calculated  $^{48}\text{Ca}$  with the addition of the isospin nonconserving Hamiltonian from [22]. This allows some

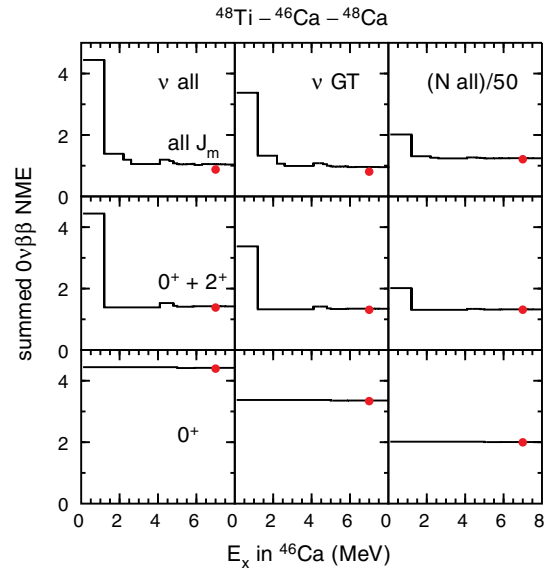


FIG. 3 (color online). Results for  $^{48}\text{Ca}$ . See caption for Fig. 2.

mixing of  $^{48}\text{Ti}$  ground state with the IAS of the  $^{48}\text{Ca}$  ground in  $^{48}\text{Ti}$ . But the mixing matrix element of 20 keV does not lead to any significant change in the result. One can also expand over intermediate states in the nucleus with two extra nucleons ( $n+2$ ), for example,  $^{78}\text{Se}$  in the case of the  $^{76}\text{Ge}$  decay. We also find that the  $J_m = 0^+$  is dominated by the ground state of the ( $n+2$ ) nucleus.

For the light neutrino, the exact TBME in the model spaces are proportional within a few percent to those obtained with the schematic interactions  $\sigma_1 \cdot \sigma_2 / r$  for GT and  $1/r$  for Fermi matrix elements. The  $1/r$  form is the well-studied Coulomb interaction whose matrix elements are dominated by a large diagonal term that conserves isospin and can only go to the double isobaric analog state of the initial nucleus. The consequence of this is that the

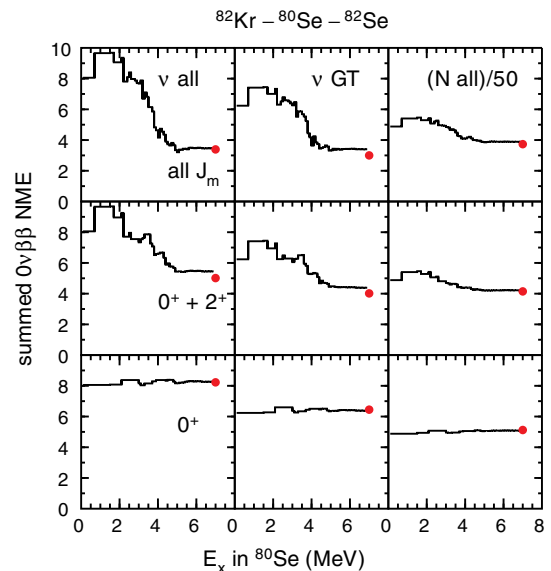


FIG. 4 (color online). Results for  $^{82}\text{Se}$ . See caption for Fig. 2.

expansion of the Fermi NME term over intermediate states in  $(A - 2)$  has positive and negative terms from that tend to cancel. Thus, the Fermi contribution is relatively small, and as observed in Figs. 2–4 the total from all terms ( $GT + F + T$ ) is within about 20% of those obtained from GT only. For the purpose of understanding the nuclear model dependencies, one can use  $\sigma_1 \cdot \sigma_2 / r$  for the interaction and study the dependence of its NME on the sum over intermediate states in the nucleus with  $(A - 2)$  nucleons. [The heavy-neutrino TBME are closely proportional to  $\delta(r)$  for Fermi and  $\sigma_1 \cdot \sigma_2 \delta(r)$  for Gamow-Teller matrix elements].

A very simple schematic diagram for the nuclear structure changes involved in double- $\beta$  decay is shown by the top row in Fig. 5. The pairing interaction enhances the two-nucleon transfers between the ground states. The bottom row of Fig. 5 shows other configurations that can be admixed into the top row either within the model space or from outside the model space. When one removes two neutrons one can also go to the deeper hole states shown by term (b) in Fig. 5. But adding two protons results in a state that has no overlap with the final state on the top left-hand side. However, such configurations are important because they will mix with the dominant ones in the top row due to the pairing interaction. Some of this mixing is already contained in the  $pf$  and  $jj44$  model spaces. But there will also be mixing with these configurations from outside the model space that will renormalize the  $0\nu\beta\beta$  NME.

It is well known that the two-nucleon transfer cross sections are enhanced by admixtures in wave function due to the pairing interaction [23,24], and it is important to test the wave functions for the nuclei involved in double- $\beta$  decay by such measurements [25]. The nuclear pairing interaction that enhances the two-particle transfer also enhances  $0\nu\beta\beta$  NME. For example, in the case of  $^{48}\text{Ca}$

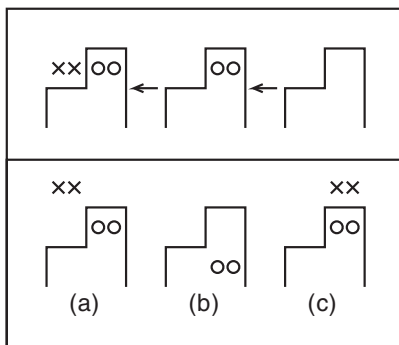


FIG. 5. Schematic diagram for the configurations involved in double- $\beta$  decay. The top row shows the configuration changes for the orbitals near the Fermi surface for double- $\beta$  decay of a nucleus with mass  $A$  through intermediate states of the nucleus with mass  $(A - 2)$ . The bottom row shows examples of important configuration admixtures to those above them in the top row. Proton occupations are shown on the left-hand side and neutron occupations are shown on the right hand side of each configuration. Crosses indicate particles and circles indicate holes.

the  $J_m = 0^+$  term is dominated by the  $0f_{7/2}$  contribution (top row of Fig. 5). There are small admixtures of the  $0f_{5/2}$ ,  $1p_{3/2}$ , and  $1p_{1/2}$  orbitals from term (c) in Fig. 5 that enhance the zero-range direct two-nucleon  $^{48}\text{Ca}$  to  $^{46}\text{Ca}$  transfer amplitude by a factor of 1.48. The (a) and (c) admixtures in Fig. 5 enhance the  $J_m = 0^+$  NME by a factors of 1.46 ( $M_N^{0\nu}$ ) and 1.24 ( $M_\nu^{0\nu}$ ).

There is also the issue of “quenching” relative to the model space. Single-particle transfer [26] and knockout [27] cross sections are usually smaller than those calculated using reaction models with shell-model spectroscopic strengths. This is attributed to short-ranged correlations [28] and particle-vibration coupling [29]. But the connection between quenching for reactions involving single-nucleon overlaps and those involving two-nucleon overlaps is not clear. Experimentally there is some indication from two-particle knockout reactions that there is quenching relative to the shell model for nuclei far from stability [30]. But one should perform knockout experiments for those nuclei involved in double- $\beta$  decay to arrive at a consistent picture with the two-particle transfer measurements in the same nuclei [25,31].

Both the pairing enhancement and quenching issues relative to the model space used in the shell model should be treated consistently in many-body perturbation theory. The first such calculations show an enhancement for the light-neutrino NME of 20% for  $^{76}\text{Ge}$  and 30% for  $^{82}\text{Se}$  [32]. Other models such as QRPA and IBM treat the pairing aspect differently. Perhaps the QRPA NME are larger than the shell-model results since more orbits are included in the pairing [15]. The effect of including admixtures from pairing correlations outside of the traditional shell model spaces used for heavier nuclei should be considered. It is well known that about half of the effective pairing interaction within the model space comes from 2nd order core-polarization admixtures (see Fig. 6 in [33]). It will be instructive to compare all models used for  $0\nu\beta\beta$  in terms of the size of total NME relative to the  $J_m = 0^+$  contribution from the  $(A - 2)$  ground state.

In summary, we have decomposed the neutrinoless double- $\beta$  decay matrix elements into sums of products over the intermediate nucleus with two less nucleons. We find that the sum is dominated by the  $J^\pi = 0^+$  ground state of this intermediate nucleus for both the light and heavy neutrino decay processes. We also explain why the light-neutrino NME is dominated by the Gamow-Teller term and show that its TBME are proportional to a simple schematic interaction. This provides new theoretical tools for comparing and improving nuclear structure models and for making connections to two-nucleon transfer and knockout reaction experiments.

Support from the NUCLEI SciDAC Collaboration under U.S. Department of Energy Grant No. DE-SC0008529 is acknowledged. M. H. and B. A. B. also acknowledge U.S. NSF Grant No. PHY-1404442.

- [1] J. C. Pati and A. Salam, *Phys. Rev. D* **10**, 275 (1974); R. N. Mohapatra and J. C. Pati, *Phys. Rev. D* **11**, 2558 (1975); W.-Y. Keung and G. Senjanovic, *Phys. Rev. Lett.* **50**, 1427 (1983).
- [2] J. D. Vergados, H. Ejiri, and F. Simkovic, *Rep. Prog. Phys.* **75**, 106301 (2012).
- [3] F. T. Avignone, S. R. Elliott, and J. Engel, *Rev. Mod. Phys.* **80**, 481 (2008).
- [4] T. Tomoda, *Rep. Prog. Phys.* **54**, 53 (1991).
- [5] E. Caurier, J. Menendez, F. Nowacki, and A. Poves, *Phys. Rev. Lett.* **100**, 052503 (2008).
- [6] M. Horoi, *Phys. Rev. C* **87**, 014320 (2013).
- [7] J. Barea and F. Iachello, *Phys. Rev. C* **79**, 044301 (2009).
- [8] J. Barea, J. Kotila, and F. Iachello, *Phys. Rev. Lett.* **109**, 042501 (2012).
- [9] T. R. Rodriguez and G. Martinez-Pinedo, *Phys. Rev. Lett.* **105**, 252503 (2010).
- [10] P. K. Rath, R. Chandra, K. Chaturvedi, P. K. Raina, and J. G. Hirsch, *Phys. Rev. C* **82**, 064310 (2010).
- [11] J. Kotila and F. Iachello, *Phys. Rev. C* **85**, 034316 (2012).
- [12] S. Stoica and M. Mirea, *Phys. Rev. C* **88**, 037303 (2013).
- [13] A. Faessler, A. Meroni, S. T. Petcov, F. Simkovic, and J. Vergados, *Phys. Rev. D* **83**, 113003 (2011).
- [14] R. A. Senkov, M. Horoi, and B. A. Brown, *Phys. Rev. C* **89**, 054304 (2014).
- [15] A. Escuderos, A. Faessler, V. Rodin, and F. Simkovic, *J. Phys. G* **37**, 125108 (2010).
- [16] R. A. Senkov and M. Horoi, *Phys. Rev. C* **88**, 064312 (2013).
- [17] F. Simkovic, R. Hodak, A. Faessler, and P. Vogel, *Phys. Rev. C* **83**, 015502 (2011).
- [18] M. Horoi and S. Stoica, *Phys. Rev. C* **81**, 024321 (2010).
- [19] M. Honma, T. Otsuka, B. A. Brown, and T. Mizusaki, *Eur. Phys. J. A* **25**, Suppl. 1, 499 (2005); *Phys. Rev. C* **69**, 034335 (2004).
- [20] M. Honma, T. Otsuka, T. Mizusaki, and M. Hjorth-Jensen, *Phys. Rev. C* **80**, 064323 (2009).
- [21] B. A. Brown and W. D. M. Rae, *Nucl. Data Sheets* **120**, 115 (2014).
- [22] W. E. Ormand and B. A. Brown, *Nucl. Phys.* **A491**, 1 (1989).
- [23] P. Decowski, W. Benenson, B. A. Brown, and H. Nann, *Nucl. Phys.* **A302**, 186 (1978).
- [24] G. Potel, A. Idini, F. Barranco, E. Vigezzi, and R. A. Broglia, *Phys. Rev. C* **87**, 054321 (2013).
- [25] S. J. Freeman *et al.*, *Phys. Rev. C* **75**, 051301(R) (2007).
- [26] B. P. Kay, J. P. Schiffer, and S. J. Freeman, *Phys. Rev. Lett.* **111**, 042502 (2013).
- [27] A. Gade *et al.*, *Phys. Rev. C* **77**, 044306 (2008).
- [28] V. R. Pandharipande, I. Sick, and P. K. A. deWitt Huberts, *Rev. Mod. Phys.* **69**, 981 (1997).
- [29] W. H. Dickhoff and C. Barbieri, *Prog. Part. Nucl. Phys.* **52**, 377 (2004).
- [30] J. A. Tostevin and B. A. Brown, *Phys. Rev. C* **74**, 064604 (2006).
- [31] A. Roberts *et al.*, *Phys. Rev. C* **87**, 051305 (2013).
- [32] J. D. Holt and J. Engel, *Phys. Rev. C* **87**, 064315 (2013).
- [33] B. A. Brown, *J. Phys. Conf. Ser.* **445**, 012010 (2013).